

Sensor Networks and Inverse Scattering

Kaviyesh Doshi
ECE Dept., Univ. of California
Santa Barbara, CA, USA
kaviyesh@ece.ucsb.edu

Shiv Chandrasekaran
ECE Dept., Univ. of California
Santa Barbara, CA, USA
shiv@ece.ucsb.edu

Patrick Dewilde
Elec. Engg. Dept., TU Delft
Netherlands
p.dewilde@ewi.tudelft.nl

ABSTRACT

We consider a wired network of analog sensors in one dimension. Each sensor measures some physical quantity and “communicates” with its adjacent neighbors. The base station can access the network by communicating with the sensors at the boundaries. We show that by making measurements at the boundary (i.e. from the first sensor) we can determine the values of the unknown field values along the entire network stably. The method is based on building an analogy with classical one dimensional inverse scattering (Helmholtz equation) for which the Chen-Rokhlin algorithm provides a highly surprising stable method for recovering the scattering parameters. Simulation results validating the scheme for thousands of sensors are presented.

Categories and Subject Descriptors

H.1.1 [Systems and Information Theory]: General Systems Theory

General Terms

Algorithms, Measurement

Keywords

Sensor Networks, Inverse Scattering, Helmholtz Equation, Chen-Rokhlin algorithm

1. INTRODUCTION

Sensors are devices which measure a certain physical quantity (e.g. temperature) and convert them into an electrical signal (e.g. voltage). The idea of a sensor network is to deploy many such sensors in a field, and through local measurements from each sensor, gather/interpolate/decipher global information about the whole field. The measurements from each of the sensors are collected and sent to a base station, where the local information is assimilated. The collection of information from each sensor is achieved in different ways

Permission to make digital or hard copies of all or part of this work for personal or classroom use is granted without fee provided that copies are not made or distributed for profit or commercial advantage and that copies bear this notice and the full citation on the first page. To copy otherwise, to republish, to post on servers or to redistribute to lists, requires prior specific permission and/or a fee.

IPSN'06, April 19–21, 2006, Nashville, Tennessee, USA.
Copyright 2006 ACM 1-59593-334-4/06/0004 ...\$5.00.

(i.e. using different protocols). The sensors for these purposes need to have more capabilities besides sensing. They also need to collect and (maybe) store data, and transmit data to either the neighbors or a base station, where the global processing is being carried out. The sensors available today are quite small in size with wide range of capabilities ([1],[2]). But, there is a power constraint for each of the sensor, since the battery on each of them will last for a finite time interval. There are few good survey papers ([3], [4], [5]), which give an overview on the sensor network problem and describe active research areas in the field.

Our objective for the sensor network in this paper is to make the sensors as inexpensive as possible by limiting their capabilities and transferring the cost of processing to the base station.

We consider a logically one dimensional, network of sensors as shown in figure (1). Here rectangular box j represents

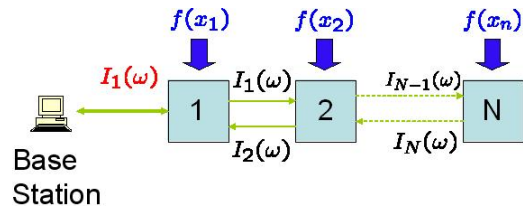


Figure 1: Schematic diagram of the proposed sensor network model

a sensor, which takes in the physical parameter $f(x_j)$ and converts it into an appropriate electrical signal. Each sensor in turn is capable of transmitting this electrical signal to its adjacent neighbors. Also, it can receive signals from its two adjacent neighbors. The base station, by sending some input signal, communicates with the first sensor at the boundary and makes some independent measurements $I_1(\omega)$. The goal of the base station is to figure out the unknowns $f(x_j)$'s from these measurements.

One way to achieve this goal would be to construct sensors so that each one of them is capable of transmitting data at unique or maybe orthogonal frequencies. But this precise carrier frequency requirement would prevent mass production and hence increase the cost of sensors. To circumvent this problem we propose a wired network of all identical sensors, each requiring only a transducer. The wired connection enables us to do away with communication costs, power constraints and localization issues. Making the base

station do most of the signal processing allows the sensor to be fabricated cheaply without any processor or memory requirement.

We have proposed the wired network with some specific applications in mind. Some of them are:

- Border/Fence monitoring ([6],[5]);
- Monitoring stress patterns in civil structures like buildings and bridges ([7]);
- Monitoring underwater cables and pipelines carrying oil/water ([6]);

Note that in all of the above applications, the fact that our sensors are wired together is not a disadvantage and it provides a low power “always on” capability. Further, extremely long bridges and pipes can require the use of thousands of sensors, and we present simulation results showing that our sensor network performs well at this scale and beyond. Furthermore the ideas that we present in this paper can be generalized to wireless networks also. Although the proposed network is logically one dimensional, we do not require that the wires run in straight lines and they can be curved to provide coverage of two dimensional areas and three dimensional volumes.

To realize such a wired network, we have taken ideas from inverse scattering theory. In particular we have modeled the one dimensional sensor network by a continuous string of unknown varying mass. It is known that if the motion of one end of such a string is observed when excited by a known force, then the unknown mass density of the string can be recovered. This was first observed by Gelfand and Levitan, who proposed an algorithm in 1955 ([8]). Chen and Rokhlin ([9]) proposed the first *stable* algorithm in 1992 and it is the algorithm that we use in this paper.

The paper is organized as follows: We first give a brief overview of inverse scattering theory along with a short description of the Chen-Rokhlin algorithm [9], and its relation with the proposed sensor network model. Then we give detailed simulation results showing the performance of the sensor network model for a wide variety of situations. In particular, we show that our proposed sensor network can operate with thousands of sensors and recover complicated field profiles from measurements carried out at the first sensor alone.

2. INVERSE SCATTERING AND ITS RELATION TO THE SENSOR NETWORK PROBLEM

Inverse scattering refers to the technique of identifying an object or some characteristics of an object by bombarding it with waves and then observing the reflected and scattered waves. There are several different research areas in the field of inverse scattering and [10] is a good survey paper. The inverse scattering problem that is closely related to our setting is the one proposed by Chen and Rokhlin in [9]. A brief description of the problem and its relevance to the sensor network problem now follows.

2.1 Inverse Scattering for the Helmholtz equation in one dimension

Consider an infinitely long string with variable mass per unit length ($q(x)$) for $x \in [0, 1]$ as shown in figure (2). The

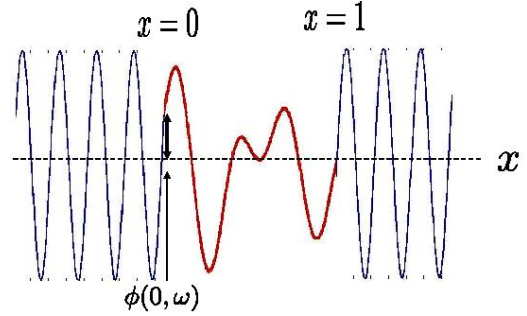


Figure 2: Inverse Scattering in One Dimension: An infinitely long string with variable mass per unit length $q(x)$ for $x \in [0, 1]$

displacement of each particle in the string is governed by the wave equation, which in the frequency domain (obtained after taking Fourier Transform) is the Helmholtz equation

$$\phi''(x, \omega) + \omega^2(1 + q(x))\phi(x, \omega) = 0, \quad (1)$$

where $\phi(x, \omega)$ is the displacement of particle at position x , and $q(x)$ is the unknown mass per unit length profile. Here $q(x) = 0$ for $x \notin [0, 1]$. The boundary conditions satisfied by $\phi(x, \omega)$ are simply the outgoing radiation boundary conditions [9]

$$\phi'(0, \omega) + i\omega\phi(0, \omega) = i2\omega, \quad (2)$$

$$\phi'(1, \omega) - i\omega\phi(1, \omega) = 0. \quad (3)$$

The goal is to observe $\phi(0, \omega)$ (for different frequencies ω), at the boundary (at $x = 0$) and extract the unknown profile $q(x)$.

To obtain $q(x)$ from the scattered data, Chen and Rokhlin solve the following non-linear system of differential equations

$$p'_+(x, \omega) = -i\omega(p_+^2(x, \omega) - (1 + q(x))), \quad (4)$$

$$p'_-(x, \omega) = i\omega(p_-^2(x, \omega) - (1 + q(x))), \quad (5)$$

$$q'(x) = \frac{2}{\pi}(1 + q(x)) \int_{-\infty}^{\infty} (p_+(x, z) - p_-(x, z)) dz \quad (6)$$

with the initial conditions

$$p_+(0, \omega) = \frac{2}{\phi(0, \omega)} - 1, \quad (7)$$

$$p_-(0, \omega) = 1, \quad (8)$$

$$q(0) = 0, \quad (9)$$

where $p_+(x, \omega)$ and $p_-(x, \omega)$ are termed as “impedances”. Here $\phi(0, \omega)$ is the measured data and $p_+(0, \omega)$ (from 7) is a function of the measured data used to solve the inverse problem.

In [9] Chen and Rokhlin established that this algorithm would reconstruct $q(x)$ in a stable manner. By stable we mean that small changes in the measured “impedance” cause small changes in the potential reconstructed by the algorithm. The only other stable algorithm for this problem that we are aware of is the one proposed by Sylvester *et. al.* ([11]).

The string problem and the sensor network model are similar at a higher level, where there is some unknown function

(along the length) to be determined by making observations at the boundary. The only difference is that the string problem is continuous, whereas the sensor network problem is discrete. We now provide a method to convert the continuous string problem to a discrete electrical network problem.

2.2 Helmholtz Equation and Sensor Networks

We need a circuit which closely resembles a string. To construct the electrical circuit we do the following:

1. Show that the current in a lossless transmission line obeys the Helmholtz equation,
2. Discretize the Helmholtz equation and obtain a lumped parameter model for the transmission line,
3. Use the lumped parameter model to construct our sensor network with an electrical circuit.

It is known that the current and voltage in the transmission line obey the Telegrapher's equation ([12]),

$$\frac{\partial V(x,t)}{\partial x} = -L(x) \frac{\partial I(x,t)}{\partial t}, \quad (10)$$

$$\frac{\partial I(x,t)}{\partial x} = -C \frac{\partial V(x,t)}{\partial t}. \quad (11)$$

Here the capacitance C is assumed to be constant along the line, while inductance L is a function of x . Differentiating equation (10) with respect to t and equation (11) with respect to x we obtain

$$\frac{\partial^2 V(x,t)}{\partial x \partial t} = -L(x) \frac{\partial^2 I(x,t)}{\partial t^2}, \quad (12)$$

$$\frac{\partial^2 V(x,t)}{\partial x \partial t} = -\frac{1}{C} \frac{\partial^2 I(x,t)}{\partial x^2}. \quad (13)$$

Comparing equations (12) and (13) we obtain the wave equation

$$L(x) \frac{\partial^2 I(x,t)}{\partial t^2} = \frac{1}{C} \frac{\partial^2 I(x,t)}{\partial x^2}. \quad (14)$$

Putting $L(x)C = 1 + q(x)$ in the above equation we get

$$\frac{\partial^2 I(x,t)}{\partial x^2} - (1 + q(x)) \frac{\partial^2 I(x,t)}{\partial t^2} = 0. \quad (15)$$

Taking Fourier Transform of the above equation we have

$$\frac{\partial^2 \hat{I}(x,\omega)}{\partial x^2} + \omega^2(1 + q(x))\hat{I}(x,\omega) = 0, \quad (16)$$

where, $\hat{I}(x,\omega)$ is the transform of $I(x,\omega)$.

To obtain the electrical circuit, we discretize the Helmholtz equation (1) using the centered difference formula

$$\hat{I}''(x_i,\omega) \approx \frac{\hat{I}(x_i - h,\omega) - 2\hat{I}(x_i,\omega) + \hat{I}(x_i + h,\omega)}{h^2},$$

we get

$$\frac{\hat{I}(x_i - h,\omega) - 2\hat{I}(x_i,\omega) + \hat{I}(x_i + h,\omega)}{h^2} + \omega^2(1 + q(x_i))\hat{I}(x_i,\omega) = 0. \quad (17)$$

At the boundaries, we discretize the outgoing radiation conditions 2 and combine it with the discrete helmholtz equa-

tion at the boundary. At $x = 0$ we get

$$\frac{\hat{I}(h,\omega) - \hat{I}(-h,\omega)}{2h} + i\omega\hat{I}(0,\omega) = 2i\omega,$$

$$\frac{\hat{I}(-h,\omega) - 2\hat{I}(0,\omega) + \hat{I}(h,\omega)}{h^2} + \omega^2(1 + q(0))\hat{I}(0,\omega) = 0.$$

Eliminating $\hat{I}(-h,\omega)$ from the above two equations, we get

$$(-2 + i2h\omega + \omega^2 h^2(1 + q(0)))\hat{I}(0,\omega) + 2\hat{I}(h,\omega) = i4h\omega. \quad (18)$$

Similarly at $x = 1$ we get,

$$\frac{\hat{I}(1+h,\omega) - \hat{I}(1-h,\omega)}{2h} - i\omega\hat{I}(1,\omega) = 0,$$

$$\frac{\hat{I}(1-h,\omega) - 2\hat{I}(1,\omega) + \hat{I}(1+h,\omega)}{h^2} + \omega^2(1 + q(1))\hat{I}(1,\omega) = 0.$$

Eliminating $\hat{I}(1+h,\omega)$ from the above two equations, we get

$$-2\hat{I}(1-h,\omega) + (2 - i2h\omega - \omega^2 h^2(1 + q(1)))\hat{I}(1,\omega) = 0. \quad (19)$$

After some algebraic manipulation, equations (17), (18) and (19) can be rewritten as

$$\left(\frac{2}{i\omega h} - 2 + i\omega h(1 + q(0))\right)\hat{I}(0,\omega) - \frac{2}{i\omega h}\hat{I}(h,\omega) = -4, \quad (20)$$

$$-\frac{2}{i\omega h}\hat{I}(x_j - h,\omega) + \left(\frac{4}{i\omega h} + i\omega 2h(1 + q(x_j))\right)\hat{I}(x_j,\omega) - \frac{2}{i\omega h}\hat{I}(x_j + h,\omega) = 0 \quad (21)$$

$$-\frac{2}{i\omega h}\hat{I}(1-h,\omega) + \left(\frac{2}{i\omega h} - 2 + i\omega h(1 + q(1))\right)\hat{I}(1,\omega) = 0. \quad (22)$$

Equations (20), (21), (22) are the Kirchoff's Voltage law (KVL) equations for the first, j th and the last loop respectively. LC ladder circuit obeying the KVL can now be formed (figure (3)). We now adapt the circuit for our

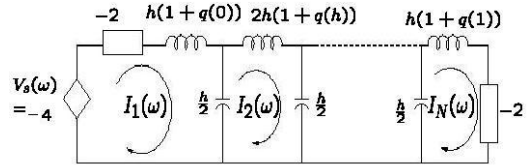


Figure 3: Electrical Circuit Realization of the 1D sensor Network Model

sensor network by identifying each inductor with a sensor, and make the special requirement that the sensed field value determines the inductor's inductance. In particular, the j th inductor with a sensed value of $q(x_j)$ has inductance $2h(1 + q(x_j))$. Such inductors can be realized using active RC circuits ([13]). To operate the sensor network, we need to make certain measurements. We supply input signals $V_s(\omega)$ (constant voltage source in frequency domain) for different

frequencies, and measure the current in the first loop, $I_1(\omega)$. Then the function $p(\omega)$ (“impedance”) is calculated as

$$p(\omega) = \frac{2}{I_1(\omega)} - 1. \quad (23)$$

To find the unknown field values $q(x_j)$, we need to find the unknown inductances from the $p(\omega)$ obtained at different frequencies. For this we can follow Chen and Rokhlin algorithm and solve equations (4)-(9). To make this feasible, Chen and Rokhlin approximated the infinite integral (6) with

$$q'(x) = \frac{2}{\pi}(1 + q(x)) \int_{-\omega_m}^{\omega_m} (p_+(x, z) - p_-(x, z)) dz, \quad (24)$$

and then use the Trapezoidal rule to discretize the integral equation.

3. IMPLEMENTATION DETAILS

We simulate figure (3) in MATLAB [14]. For the forward problem, we choose different profiles for $q(x)$, send an input voltage signal, which is an impulse in time (and hence a constant in frequency), and measure the current ($I_1(\omega)$) in the first loop. It is equivalent to solving a linear system of equations obtained by writing the KVL equations. To add noise, we simply put a resistor in each loop. The value of the resistor is a uniform random number in $[0, .1]$, which is of the order of (or greater than) the product of $LC(= h^2)$. Once we have $I_1(\omega)$, we form the “impedance” function as in (23), and solve the system of ODE’s (4) - (9), with (6), and (7) replaced by (24), and (23) respectively. We use MATLAB’s ode23s solver for solving the system of differential equations. The integration in (24) is approximated using the trapezoidal sum.

Once we have the reconstructed profile $\hat{q}(x)$, we calculate the error as

$$e(x) = q(x) - \hat{q}(x).$$

In the captions of each figure, we show two different norms of errors:

- $\|e(x)\|_\infty = \max_i e(x_i)$, which is the maximum reconstruction error made by a sensor.
- $\|e(x)\|_2 = \left(\frac{1}{\sqrt{N}}\right) \sqrt{(\sum_i e(x_i)^2)}$, which is the root mean squared reconstruction error.

4. RESULTS

Our goal is to show that it is possible to recover the unknown sensed profile by making measurements at the boundary. According to [9], the inverse algorithm works the best when the unknown profile is smooth, and the error tends to zero as one takes samples at higher frequencies. The following observations are verified through plots:

- The reconstruction error decreases up to a point as we increase the maximum frequency (ω_{max}). Beyond that the error persists, which is due to the fact that we have used different models for the forward and inverse problem.
- The algorithm scales quite well with the number of sensors, and the error does not blow up with the increase in the number of sensors.

- The reconstruction algorithm is able to resolve two peaks separated by some distance.
- Although [9] does not have proof for detecting non-smooth profiles, the algorithm does a good job reconstructing it. We show this by using profiles, which are piecewise smooth, and piecewise non-smooth.

For all the plots shown below, the x-axis represents the spatial axis along which the sensors are aligned, and the y-axis is the sensed field value, as well as the absolute value of the reconstructed potential.

4.1 Smooth Profile

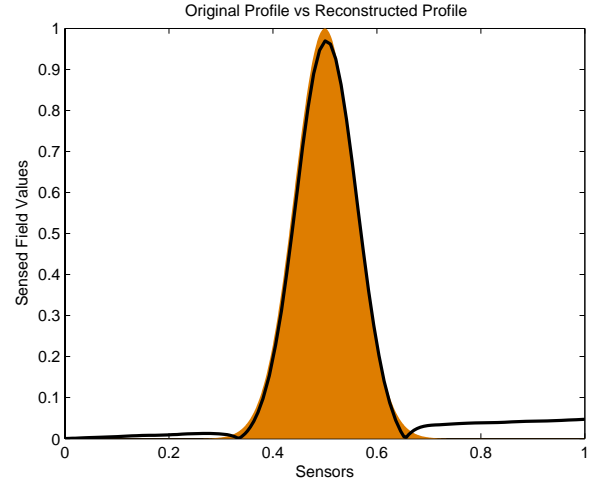


Figure 4: Smooth $q(x)$: 1,000 sensors, $\omega_{max} = 30$ rad/sec. Noisy resistor is uniformly chosen from the interval $[0,0.1]$. $\|error\|_2 = 0.0295$, $\|error\|_\infty = 0.0552$. The solid line corresponds to the reconstructed profile and the area plot corresponds to the original profile.

Here we show that if the L_i ’s (the spatially distributed sensed value) vary smoothly then it is possible to recover them to a high degree of accuracy. We show experimental results for different ω_{max} and show that the recovered profile follows the original profile closely as we increase ω_{max} . We choose $q(x)$ as

$$q(x_i) = \exp\left(-\left(\frac{x_i - .5}{\sigma}\right)^2\right)$$

where $\sigma = \frac{1}{8}\sqrt{\log_{10}(e)}$ and $L(x_i)$ is obtained from $q(x_i)$ as shown in figure (3). In most practical situation, one would expect high correlation between adjacent sensed values and hence the smoothness requirement would be satisfied most of the time. As can be seen in figure (4), the inverse algorithm is successful in reconstructing the $q(x)$; i.e. it follows the original profile quite closely. Figure (5) shows the plot of impedance (as a function of frequency), which is supplied to inverse algorithm (equation (23)).

We don’t see significant improvement when the frequency is raised from 30 to 60 rad/sec (figures (4) and (6)). This is due to the fact that, the forward problem (i.e. collecting the data $I_1(\omega)$) is in discrete domain (i.e. obtained through

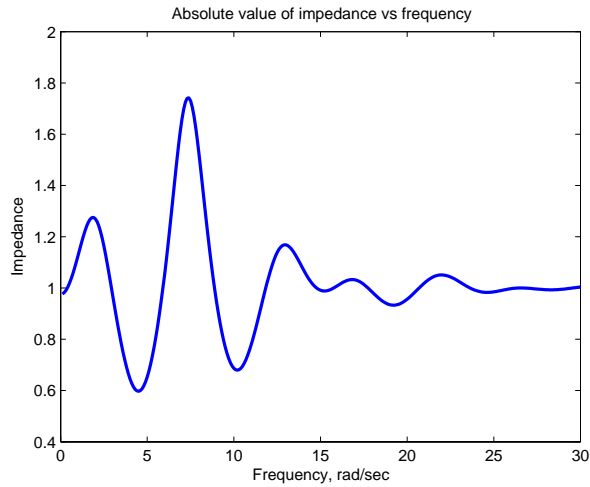


Figure 5: Impedance profile for figure (4). 1,000 sensors, $\omega_{max} = 30$ rad/sec.

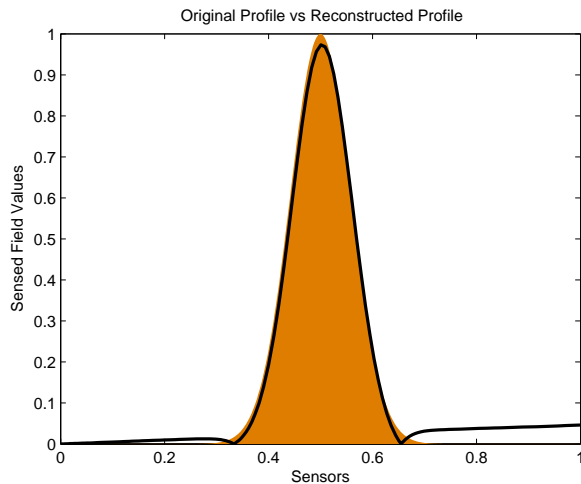


Figure 6: Smooth $q(x)$: 1,000 sensors, $\omega_{max} = 60$ rad/sec. Noise is a uniform random number between $[0,0.1]$. $\|error\|_2 = 0.0291$, $\|error\|_\infty = .0543$. The solid line corresponds to the reconstructed profile and the area plot corresponds to the original profile.

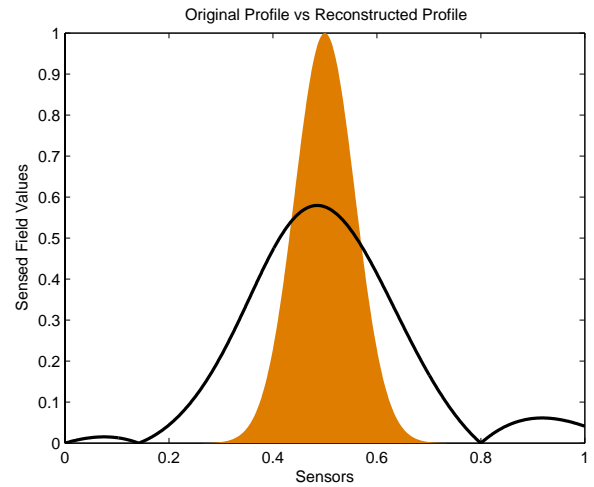


Figure 7: Smooth $q(x)$: 1,000 sensors, $\omega_{max} = 5$ rad/sec. Noise is a uniform random number between $[0,1]$. $\|error\|_2 = 0.1695$, $\|error\|_\infty = .4242$. The solid line corresponds to the reconstructed profile and the area plot corresponds to the original profile.

a lumped parameter model), whereas the reconstruction algorithm (the inverse problem - equations (4), (5), and (6)) is in continuous domain.

On other hand figure (7) indicates that if we decrease the maximum frequency of experiments, the performance of the inverse algorithm deteriorates.

4.2 Step profile

In practice, step profile would correspond to a case, where the sensed value is among a few quantized levels. Although Chen-Rokhlin algorithm requires smooth potential, it is able to reconstruct a piecewise smooth profile to great accuracy. Figure (8) corresponds to the case where the number of quantization level is more than two, whereas figure (9) corresponds to the case where only one bit of information (either 0 or 1) is transmitted. The reconstructed profile for both the cases give a reasonable picture of the quantized field values. As shown in figure (10), when the maximum frequency is increased to 75 rad/sec, we see that the error in reconstruction further decreases.

4.3 Resolution

To test the inverse algorithm for its resolution ability we considered two cases. Figure (11) indicates successful resolution of two peaks separated by some distance, and the inverse algorithm works quite well even when the distance between the two peaks is reduced (figure (12)).

Figure (13) indicates successful resolution of a highly localized peak.

4.4 Scalability

The number of sensors is increased to 10,000 now. As shown in figures (14) and (15), the inverse algorithm was able to detect the profile successfully, thereby indicating the scalability of the algorithm. Also, the noise level for figure (15) is reduced by an order of magnitude resulting in a better reconstruction.

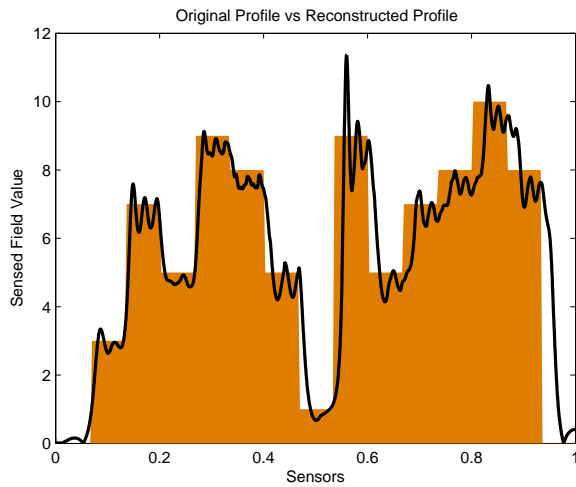


Figure 8: Step profile: 300 sensors, $\omega_{max} = 50$ rad/sec. Noise is a uniform random number between $[0,1]$. $\|error\|_2 = 1.6127$, $\|error\|_\infty = 7.7227$. The solid line corresponds to the reconstructed profile and the area plot corresponds to the original profile.

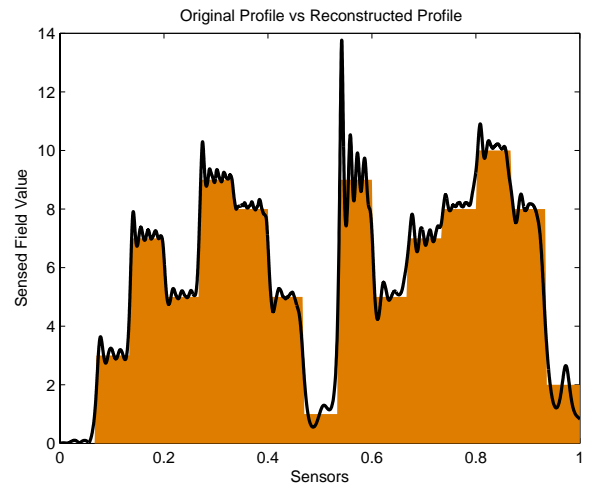


Figure 10: Step profile: 300 sensors, $\omega_{max} = 75$ rad/sec. Noise is a uniform random number between $[0,1]$. $\|error\|_2 = .6508$, $\|error\|_\infty = 3.9715$. The solid line corresponds to the reconstructed profile and the area plot corresponds to the original profile.

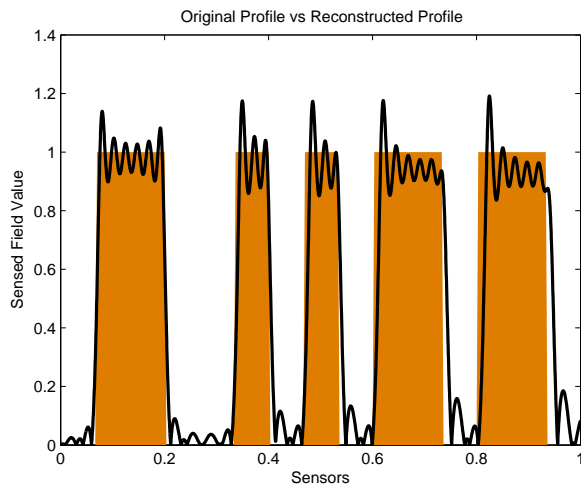


Figure 9: Step profile: 300 sensors, $\omega_{max} = 100$ rad/sec. Noise is a uniform random number between $[0,1]$. $\|error\|_2 = .2118$, $\|error\|_\infty = 1.0033$. The solid line corresponds to the reconstructed profile and the area plot corresponds to the original profile.

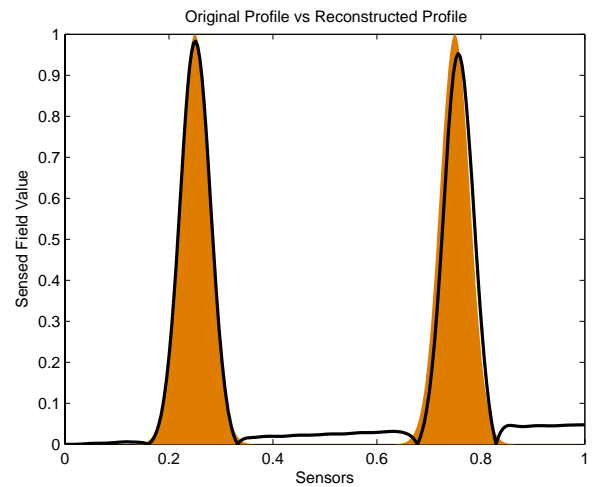


Figure 11: Resolution: 1,000 sensors, $\omega_{max} = 50$ rad/sec. Noise is a uniform random number between $[0,1]$, $\|error\|_2 = 0.0487$, $\|error\|_\infty = 0.1913$. The solid line corresponds to the reconstructed profile and the area plot corresponds to the original profile.

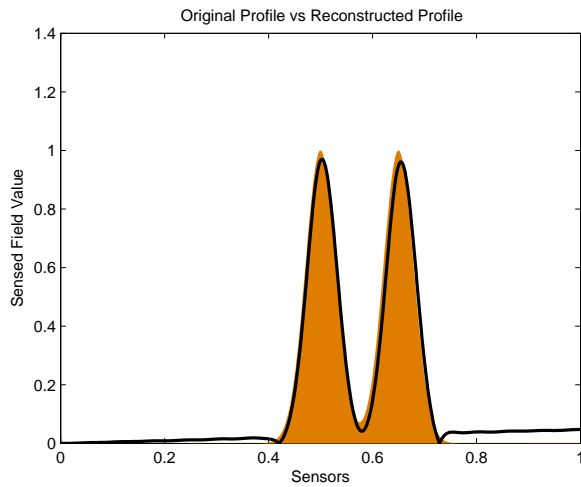


Figure 12: Resolution: 1,000 sensors, $\omega_{max} = 50$ rad/sec. Noise is a uniform random number between $[0,1]$, $\|error\|_2 = 0.0426$, $\|error\|_\infty = 0.1393$. The solid line corresponds to the reconstructed profile and the area plot corresponds to the original profile.

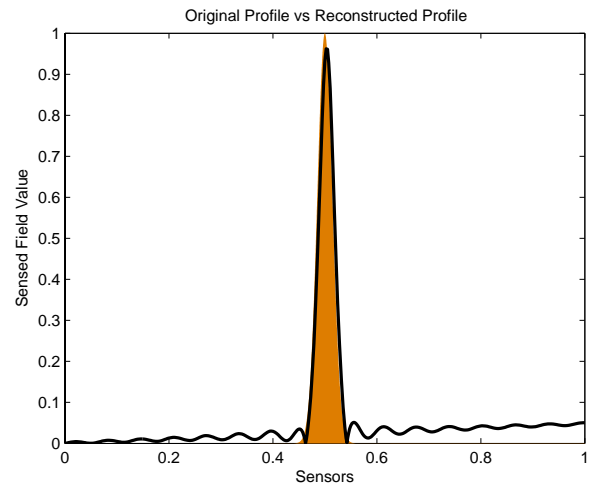


Figure 14: Scalability: 10,000 sensors, $\omega_{max} = 50$ rad/sec. Noise is a uniform random number between $[0,1]$. $\|error\|_2 = 0.0395$, $\|error\|_\infty = 0.178$. The solid line corresponds to the reconstructed profile and the area plot corresponds to the original profile.

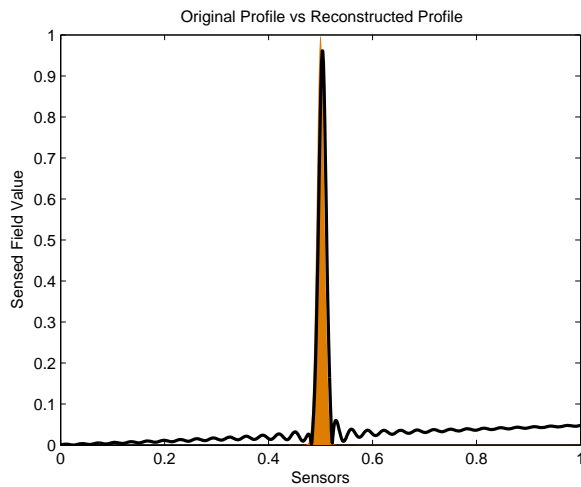


Figure 13: Resolution: 1,000 sensors, $\omega_{max} = 100$ rad/sec. Noise is a uniform random number between $[0,1]$. $\|error\|_2 = 0.0481$, $\|error\|_\infty = 0.32$. The solid line corresponds to the reconstructed profile and the area plot corresponds to the original profile.

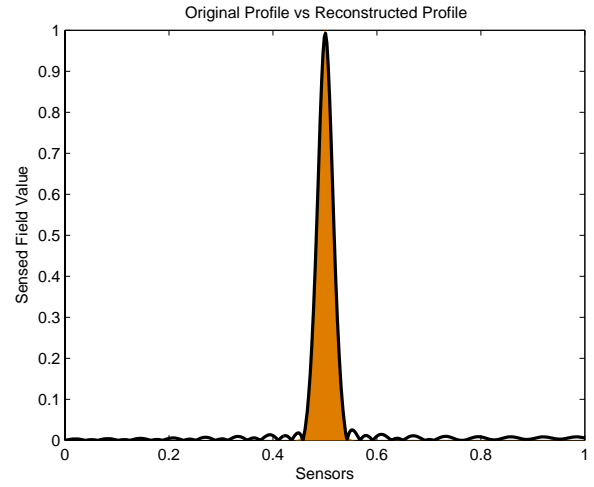


Figure 15: Scalability: 10,000 sensors, $\omega_{max} = 50$ rad/sec. Noise is a uniform random number between $[0,.01]$, $\|error\|_2 = 0.0101$, $\|error\|_\infty = 0.0497$. The solid line corresponds to the reconstructed profile and the area plot corresponds to the original profile.

4.5 Non-smooth profiles

Although for most practical cases, the sensed profile will be smooth, we would like to see if the inverse algorithm is able to reconstruct non-smooth profiles. We used the function

$$q(x_i) = |0.5(\sin(2k\pi x_i))^{-25}|$$

which has infinite derivative (and hence not piecewise smooth) for finite values of x . The parameter k controls the number of lobes. As shown in figure (16), Chen-Rokhlin algorithm is

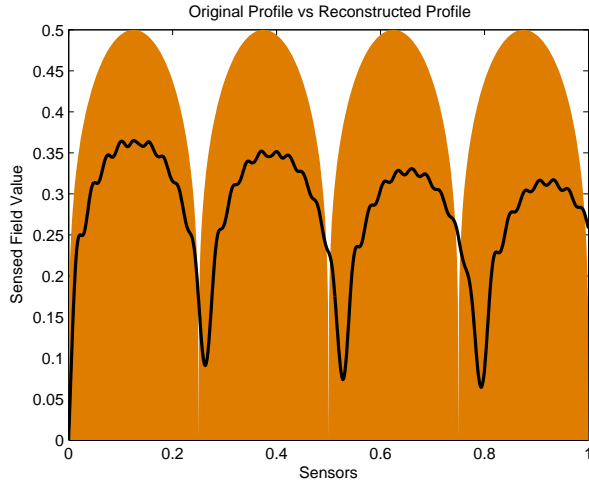


Figure 16: Piecewise non-smooth: $q(x_i) = |0.5(\sin(4\pi x_i))^{-25}|$, 1,000 Sensors, $\omega_{max} = 100$ rad/sec. Noise is a uniform random number between $[0,1]$. $\|error\|_2 = .1643$, $\|error\|_\infty = .3629$. The solid line corresponds to the reconstructed profile and the area plot corresponds to the original profile.

able to detect the shape of the potential along with number of lobes.

5. CONCLUSION AND FUTURE WORK

In this paper we have proposed a novel model of sensor networks. Using an inverse scattering algorithm, we were able to recover the unknown field values by making measurements only at the boundary. This method enables us to construct sensors cheaply and transfer the cost of signal processing to the base station. The simulation results indicate a stable recovery of different profiles and a high degree of scalability. The algorithm is stable in the sense that the error does not blow up either due to increasing the number of sensors or due to noise in the network.

In future we will address the following issues:

- Although, here the noise is modeled as resistors in series with the sensors, other possibilities also exist. Ideally a noise model should include all possible sources of noise, e.g. measurement noise of each sensor, measurement noise of the impedance measuring device, noise causing attenuation in the signal etc.
- The plots for the case of smooth field values show a presence of a finite error between the actual field values and the recovered field values. The error does not

decrease by taking samples of impedance at higher frequencies as predicted by the inverse scattering algorithm [9]. It is due to the discrepancy in the two (forward and inverse) models, i.e. (in the forward model) impedance is calculated using a discrete circuit, while (in the inverse model) the impedance data is supplied to a continuous inverse scattering algorithm. We believe that this error can be reduced by developing an inverse algorithm in discrete domain.

- In the paper, the simulations are performed in frequency domain. In real world applications, it is more likely that the experiment is performed in time domain. Hence one needs to consider other issues like the settling time of the circuit, operation of the circuit in stable fashion, etc.
- Although the algorithm described in the paper can be used for two dimensional area and three dimensional volume, we will consider better models for sensing in two dimensional field.

6. REFERENCES

- [1] Crossbow technology inc. [Online]. Available: <http://www.xbow.com/index.aspx>
- [2] Smart dust. [Online]. Available: <http://robotics.eecs.berkeley.edu/~pister/SmartDust/>
- [3] M. Tubaishat and S. Madria, "Sensor networks: An overview," *IEEE Potentials*, vol. 22, no. 2, pp. 20–23, April-May 2003.
- [4] A. Ahmed and M. R. Eskicioglu, "Current researches on sensor networks," Telecommunication Research Labs, Winnipeg, Manitoba, Canada, Tech. Rep. TR-01-06/04, 2004.
- [5] A. Bharathidasan and V. A. S. Ponduru, "Sensor networks: An overview." [Online]. Available: <http://wwwcsif.cs.ucdavis.edu/~bharathi/sensor/survey.pdf>
- [6] Bei security. [Online]. Available: <http://www.beisecurity.com/products.html>
- [7] Smart buildings admit their faults. [Online]. Available: <http://www.coe.berkeley.edu/labnotes/1101smartbuildings.html>
- [8] I. Gel'fand and B. Levitan, "On a determination of differential equation from its spectral function," *American Mathematical Society Translation, Series 2*, vol. 1, pp. 253–304, 1955.
- [9] Y. Chen and V. Rokhlin, "On the inverse scattering problem for the helmholtz equation in one dimension," *Inverse Problems*, vol. 8, no. 3, pp. 365–391, 1992.
- [10] D. Colton, J. Coyle, and P. Monk, "Recent developments in inverse acoustic scattering theory," *SIAM Review*, vol. 42, no. 3, pp. 369–414, 2000.
- [11] J. Sylvester, D. Winebrenner, and F. Gylys-Colwell, "Layer stripping for helmholtz equation," *SIAM Journal of Applied Mathematics*, vol. 56, no. 3, pp. 736–754, June 1996.
- [12] M. R. Wohlers, *Lumped and distributed passive networks*. Academic Press, New York, 1969.
- [13] M. S. Ghausi and K. R. Laker, *Modern Filter Design: Active RC and Switched Capacitor*. Prentice-Hall Inc.: Englewood Cliffs, NJ, 1981.
- [14] The mathworks. [Online]. Available: <http://www.mathworks.com/>